Computational Fluid Dynamics Simulation of Injection Mixer for CNG Engines

Yvonne S. H. Chang, Z. Yaacob and R. Mohsin

Abstract— The poor mixing in gaseous injection mixers is one of the culprits for unsatisfactory engine performance and lethal exhaust emissions. Thus, effect of injection frequency on the mixing in Throttle Body Injection Mixer (TBIM) for a CNG motorcycle was studied in this work through Computational Fluid Dynamics (CFD) simulation. Injection frequencies of 1, 2, 4, 5 and 7 injections per engine cycle had been investigated using the RNG k-ε turbulent model. CFD results revealed a significant effect of various injection frequencies on the hydrodynamics of air and fuel in TBIM. It was found that the injection frequency of 4 injections per engine cycle was the most optimum one throughout the case studies.

***Index Terms*—** Injection frequency; Throttle Body Injection Mixer (TBIM); Computational Fluid Dynamics (CFD)

I. Introduction

One of the problems of gaseous mixers is the ability to prepare a homogeneous mixing of air and fuel at a specific air-fuel ratio prior to entering the engine. This issue, if not being taking care of, may result in high BSFC and high exhaust emissions. Hence, investigation was conducted to enhance the mixing in Throttle Body Injection Mixer (TBIM), which is the new generation of mixer for a CNG motorcycle, through CFD simulation. The purpose of this study is to prepare a homogeneous mixing of air and fuel at a specific air-fuel ratio before entering the engine.

Yvonne S. H. Chang is currently with Universiti Teknologi PETRONAS, Chemical Engineering Department, Bandar Seri Iskandar, 31750 Tronoh, Perak, Malaysia (phone: +60-5-3687644; fax: +60-5-3656176; e-mail: yvonne_csh@yahoo.com).

Z. Yaacob is with Universiti Teknologi Malaysia, Gas Engineering Department, UTM Skudai, 81310 Skudai, Johor, Malaysia (e-mail: zyaacob@gmail.com).

R. Mohsin is with Universiti Teknologi Malaysia, Gas Engineering Department, UTM Skudai, 81310 Skudai, Johor, Malaysia (e-mail: drrahmat@gmail.com).

Recent research that has integrated CFD simulation into the design of IC engines include the optimisation of air-fuel mixing in a direct injection spark ignition (DISI) engine [1], measurement of in-cylinder mixing rate [2], simulation of the interaction of intake flow and flow spray in a DISI engine [3], simulation and control of CNG engines [4], optimisation of air-fuel mixing homogeneity and performance improvements of a stratified-charge direct injection combustion system [5] and so forth. In this research, CFD simulation was conducted to determine and optimise the injection frequency in TBIM for the best air-fuel mixing prior to entering the engine.

As yet, the research works available in improving the mixing quality of injection-type mixers include the study of geometry design, injection to crossflow velocity ratio, crossflow swirl strength, injection timing, wall-impinging injection with a bump placed in the injection impingement region, injection position and injection inclination angles [6]. Study on the effect of various injection frequencies on mixing is still rarely seen. Hence, to ensure the simulation condition was compatible with the actual engine operating condition, experimental work was conducted at the outset of the research to obtain the engine suction pressure in the intake manifold for each case study. The data was then verified thoroughly through previous work before applying it in the CFD simulation [6]. The same research methodology had been carried out to investigate the effect of various injection inclination angles on the mixing in TBIM and its results were found to be consistent with previous work [6].

Concern over the consistency of CFD simulation results with the corresponding theoretical and experimental findings has been an issue since the last few years. Nevertheless, the performance of CFD simulation has shown a dramatic improvement after consecutive refinements over the years. Ref [3] claimed that CFD simulation was an equal partner with pure theory and pure experiment in the analysis and solution of fluid dynamic problems. Other researches such as [1], [5] and [7] have also proven the validity of the results obtained through CFD simulation. In addition, CFD simulation of the single-phase mixing problems has been well-established [3]. Thus, the results obtained in this simulation work can be utilised with a very high level of confidence.

II. Computational Fluid Dynamics Simulation of Throttle Body Injection Mixer

A schematic diagram of TBIM is shown in Fig. 1. It consists of a throttle valve, fuel injector, reducer and intake manifold. The amount of air entering TBIM is manipulated by the opening of throttle valve whereas the amount of fuel

required is controlled by the fuel injector. The air and fuel are mixed in TBIM before entering the engine. In this work, the fuel was injected at various injection frequencies, i.e. 1, 2, 4, 5 and 7 injections per engine cycle to study its effect on the mixing in TBIM. CFD simulation of TBIM commenced with model meshing, followed by the optimisation of grids and selection of turbulent model before starting the computation.

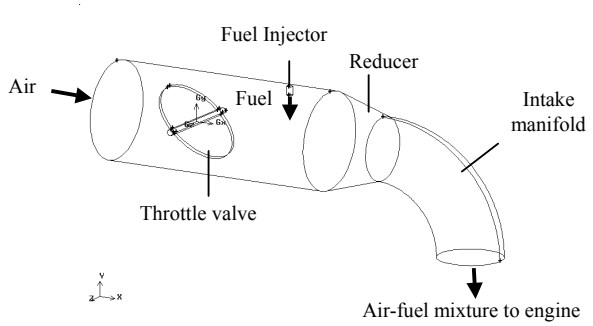

Fig. 1: Outline of TBIM

II.1 Model Meshing

Owing to the symmetrical attribute of TBIM and consideration of computational expense, only a symmetrical portion of TBIM was modelled (Fig. 2). By doing so, the simulation would yield an output for the whole of TBIM at 10% of the computational time.

There are two types of grids to choose from for model meshing, i.e. structured and unstructured grids. The first one is composed of hexahedral elements while the latter one consists of tetrahedral elements. A general rule of thumb is to apply the structured grids on simple geometries and the unstructured grids on complex geometries. For a complex geometry such as the main body of TBIM, which consists of a throttle valve and an injector, the unstructured grids were applied (Fig. 2). On the other hand, the structured grids were chosen for simple geometries like the intake manifold (an arched cylinder) and the reducer (a pinnacle-less cone) that connects the main body of TBIM with the intake manifold (Fig. 2).

A general guideline of model meshing is to always mesh the more critical domains (i.e. high velocity, high pressure or pressure drop flow fields) in advance of the less critical ones. For TBIM, the more critical domains include the regions around the openings of throttle valve and the injector (Fig. 2). The fineness of grid applied increases with the criticalness of a domain. After TBIM was appropriately meshed, the boundary conditions of TBIM were identified for the air inlet, fuel outlet, mixture outlet and the symmetry plane (Fig. 2). Boundary conditions of 'pressure inlet' and 'mass flow inlet' were selected for the air inlet and fuel outlet, whereas the mixture outlet and the symmetry plane were given the boundary condition of 'wall'. These choices of boundary condition were depending on the available data and also the data required from the simulation.

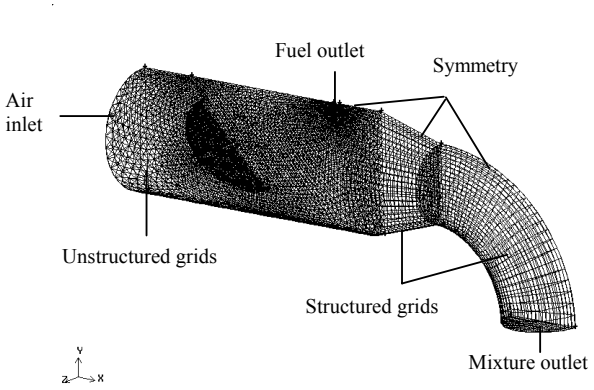

Fig. 2: Computational mesh system and boundary conditions of TBIM for CFD simulation

II.II Optimisation of Grid

After model meshing, the grids on TBIM were optimised. This step is essential as it helps to minimise the numerical errors in computation during the simulation work. The intention of this optimisation process is to determine an acceptable grid size that is able to reach a balance between the amount of computing time and the accuracy in the solution of flow variables.

Fig. 3 exhibits the velocity contours captured at the axisymmetric plane of TBIM which utilise three different total numbers of grid cells, i.e. 20149, 41263 and 61840 cells. It is obvious that the velocity contours of 20149 grid cells are different from those of 41263 and 61840 grid cells. The latter two are, however, in a good agreement with each other. In consideration of the less computing time involved, TBIM with a total number of 41263 grid cells was selected over the one with 61840 grid cells.

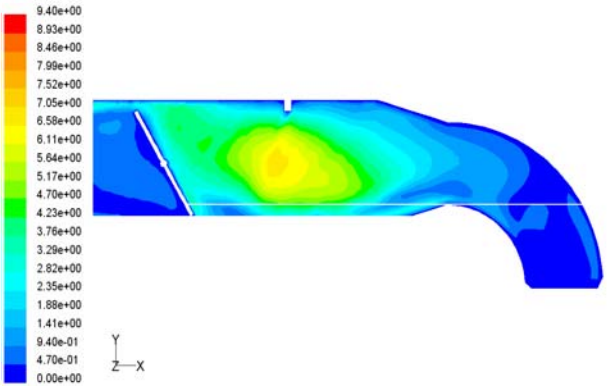

(a)

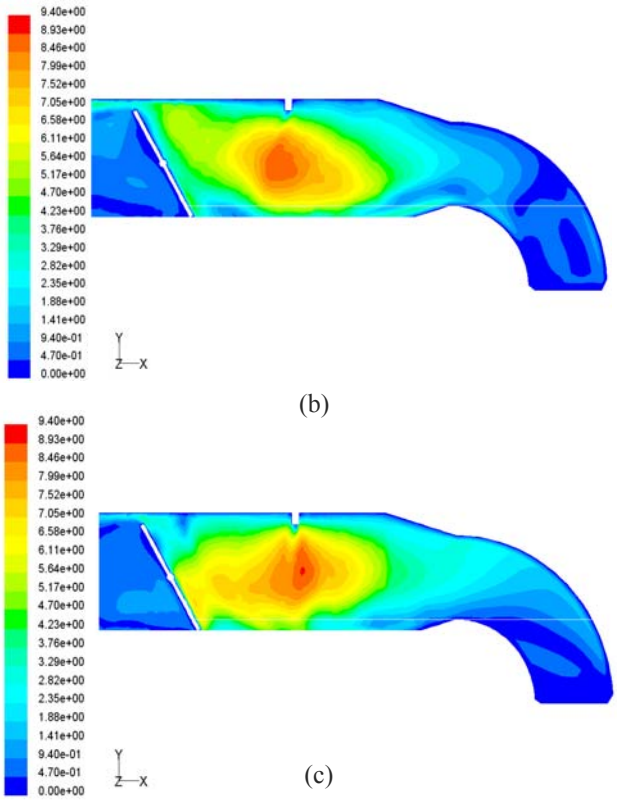

Fig. 3: Velocity contours of TBIM with a total number of (a) 20149, (b) 41263 and (c) 61840 grid cells

II.III Determination of Turbulent Model

Among all the turbulent models, the κ-ε model was selected in this work because it is the most widely used and validated one in terms of consistency and reliability [8]-[9]. There are three types of κ-ε model, namely the Standard κ-ε model, Renormalization Group (RNG) κ-ε model and Realizable κ-ε model. The major differences between these models are the methods in calculating the turbulent viscosity, turbulent Prandtl numbers and the generation and destruction terms in the ε equation.

The Standard κ-ε model is the most extensively used and validated turbulent model among all the κ-ε models. It has achieved notable successes in calculating a wide variety of thin shear layer flows. Nevertheless, it is reported not to perform well in some important cases like flows with large extra strains (e.g. curved boundary layers, swirling flows) and rotating flows [9]. The RNG κ-ε model, on the other hand, is similar in form to the Standard κ-ε model, except for some added refinements to improve the accuracy for rapidly strained flows. As for the Realizable κ-ε model, initial studies have shown that it is the best κ-ε model in solving fluid dynamic problems. However, the Realizable κ-ε model has yet to prove in exactly which instances it consistently outperforms the RNG κ-ε model. According to [10] and [1], the RNG k-ε model showed a better agreement with experiments than the other κ-ε models, particularly in predicting the gaseous penetration of both free and confined injection. It is more responsive to rapid strain and streamlines curvature relative to the other two κ-ε models. In addition, it takes into account the effect of swirl on turbulence, thus enhancing the accuracy for swirling flows. Therefore, for a rapidly strained gaseous flow with a confined injection in TBIM, the RNG κ-ε model was preferred. The transport equations of RNG κ-ε used in this work are as follows:

$$\frac{\partial}{\partial t}(\rho k)+\frac{\partial}{\partial x_i}(\rho k u_i)=\frac{\partial}{\partial x_j}\left(\alpha_k \mu_{eff}\frac{\partial k}{\partial x_j}\right)+G_k+G_b-\rho\varepsilon-Y_m+S_k \quad (1)$$

$$\frac{\partial}{\partial t}(\rho \varepsilon)+\frac{\partial}{\partial x_i}(\rho \varepsilon u_i)=\frac{\partial}{\partial x_j}\left(\alpha_\varepsilon \mu_{eff}\frac{\partial \varepsilon}{\partial x_j}\right)+C_{1\varepsilon}\frac{\varepsilon}{k}(G_k+C_{3\varepsilon}G_b)-C_{2\varepsilon}\rho\frac{\varepsilon^2}{k}-R_e+S_e \quad (2)$$

where ρ is the fluid density, k is the kinetic energy, ε is the dissipation rate, u is the mean velocity, μ_{eff} is the effective viscosity, α_k is the inverse effective Prandlt number for the k term, α_ε is the inverse effective Prandlt number for the ε term, G_k is the generation of turbulent kinetic energy due to mean velocity gradients, G_b is the generation of turbulent kinetic energy due to buoyancy, Y_m is the contributions of the fluctuating dilation in compressible turbulence to the overall dissipation rate, S_k and S_ε are the user defined source terms for k and ε, respectively. R_ε is an additional term in the RNG κ-ε model which is modelled by:

$$R_\varepsilon=\frac{C_\mu \rho \eta^3\left(1-\eta/\eta_0\right)\varepsilon^2}{1+\beta\eta^3}\cdot\frac{\varepsilon^2}{k} \quad (3)$$

where $\eta = S_k/\varepsilon$, $\eta_0 = 4.38$ and $\beta = 0.012$ [8]. By substituting (3) into (2), the (2) can be rewritten as:

$$\frac{\partial}{\partial t}(\rho \varepsilon)+\frac{\partial}{\partial x_i}(\rho \varepsilon u_i)=\frac{\partial}{\partial x_j}\left(\alpha_\varepsilon \mu_e\frac{\partial \varepsilon}{\partial x_j}\right)+C_{1e}\frac{\varepsilon}{k}(G_k+C_{3\varepsilon}G_b)-C_{2e}^*\rho\varepsilon^2/k \quad (4)$$

where the constants $C_{1e} = 1.42$ and $C_{2e} = 1.68$ [8].

III. AIR FUEL MIXING AND HOMOGENEITY

In this work, air and fuel were delivered into TBIM at stoichiometric air-fuel ratio, i.e. 17.3:1. Nevertheless, the air-fuel ratio of the mixing before entering the engine could be differed from this value owing to poor mixing. A good mixing would give a stoichiometric mass fraction of methane ($M_{ch4.s}$) locally throughout the mixing region. The $M_{ch4.s}$ was calculated as follows:

$$M_{ch4.s} = 1/18.3 = 0.0546$$

In order to determine the quality of mixing in TBIM, the mass fraction of methane (M_{ch4}) throughout the axial length of TBIM was investigated using the histogram as shown in Fig. 4. During the investigation, M_{ch4} with the highest frequency (M_{hf}) was retrieved from each histogram. The closer the M_{hf} to the $M_{ch4.s}$, the better the mixing quality obtained and vice versa.

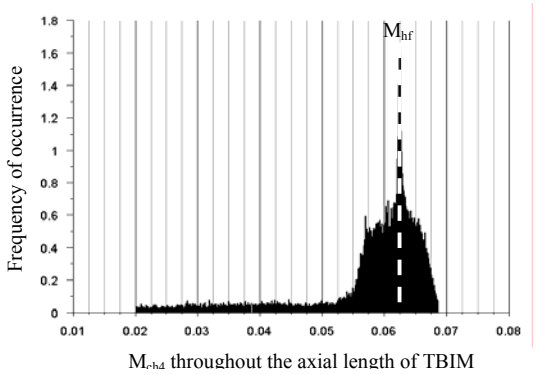

Fig. 4: Histogram of M_{ch4} used to determine M_{hf}

In addition, the quality of mixing was also investigated through the mixing homogeneity (H_m) in TBIM. The H_m was defined as the ability of air and fuel to mix with a uniform M_{ch4} in TBIM. To justify the H_m more effectively, the quality of H_m had been standardized and graded according to the number of contours of M_{ch4} in the mixing region (Fig. 5). The best H_m, i.e. Grade A, was exhibited by merely one contour of M_{ch4}. However, if it happened to have two contours of M_{ch4} instead of one, Grade B would be considered. As for Grade C, it was signified by a total of three contours of M_{ch4} in the mixing region concerned. Finally, the worst H_m, which had four or more contours of M_{ch4} in the mixing region concerned, was represented by Grade D.

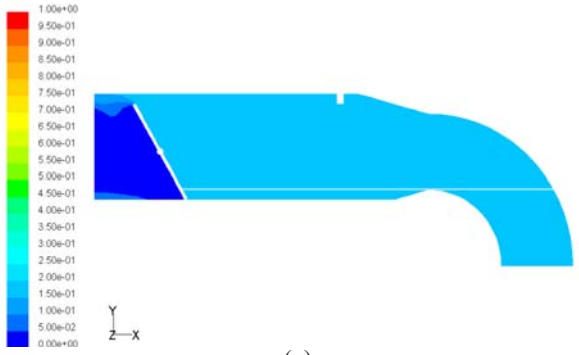

(a)

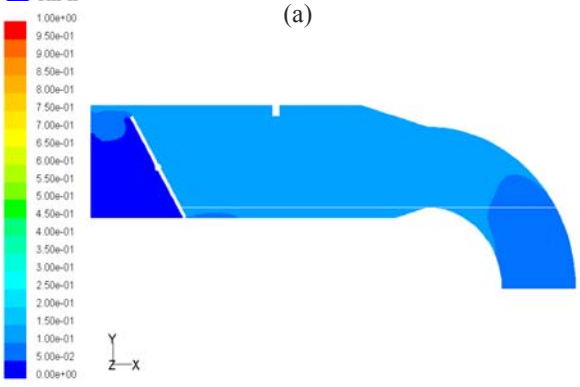

(b)

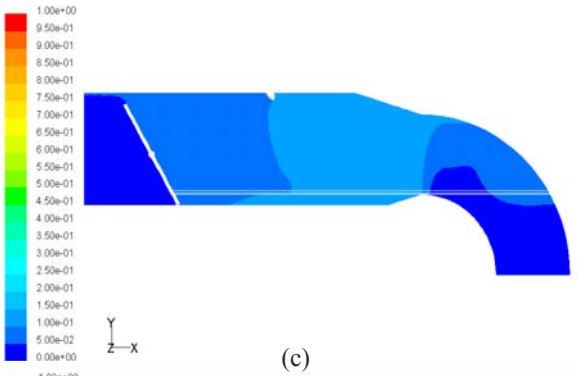

(c)

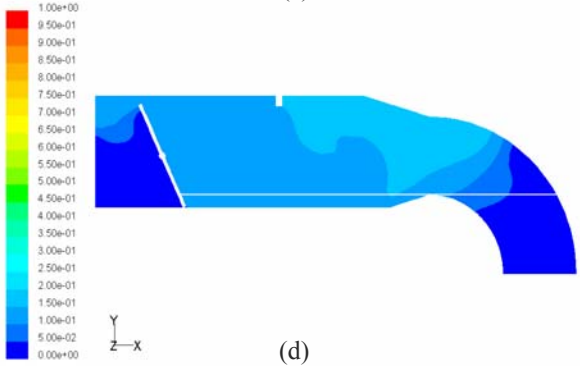

(d)

Fig. 5: Standardization of quality of H_m with (a) Grade A, (b) Grade B, (c) Grade C and (d) Grade D

IV. EFFECT OF INJECTION FREQUENCIES ON M_{HF}

Fig. 6 shows the effect of various injection frequencies on M_{hf} throughout the case studies at different engine speeds and throttle openings. The injection frequencies studied were 1 (1if), 2 (2if) and 4 (4if) injections per engine cycle. On the whole, the M_{hf} at 4if showed the lowest value compared to the other two smaller injection frequencies. The lower the M_{hf}, the closer it was to the $M_{ch4.s}$, and thus the better the mixing quality. Hence, injection frequency at 4if exhibited the best mixing quality in TBIM.

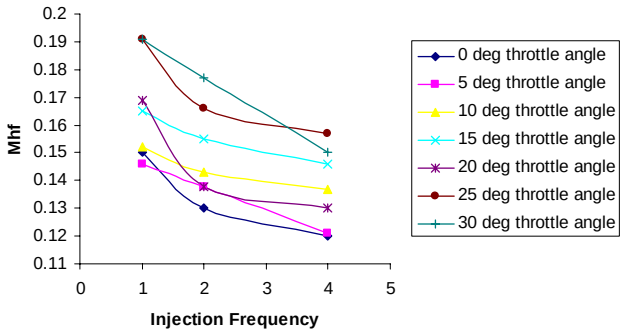

(a)

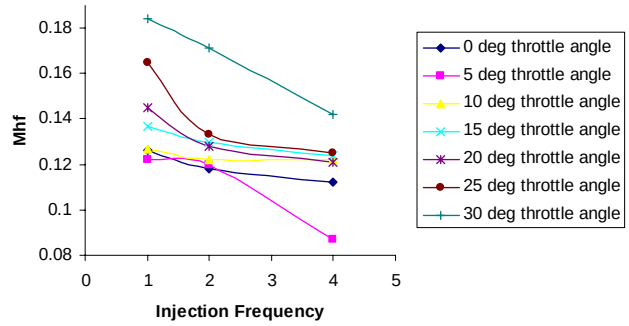

(b)

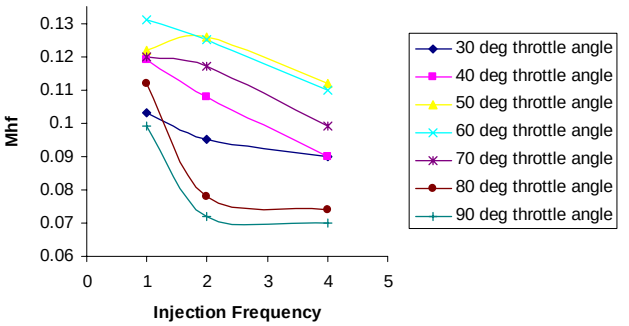

(c)

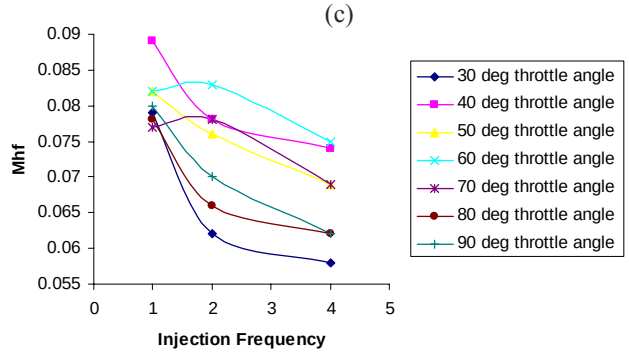

(d)

Fig. 6: M_{hf} vs injection frequency at (a) 1680 rpm, (b) 2160 rpm, (c) 4500 rpm and (d) 7200 rpm

The effect of injection frequency on the mixing in TBIM was strongly related to the sustainability of injection momentum and mixing energy. By applying more than one injection per engine cycle in the TBIM, a much greater turbulent intensity could be achieved as the injection took place intermittently [11]. Hence, the sustainability of injection momentum and mixing energy were increased. In this way, the mixture was able to mix thoroughly owing to the adequate mixing energy provided periodically. As a result, the M_{hf} decreased with increasing injection frequencies.

V. EFEECT OF INJECTION FREQUENCIES ON H_M

Unlike the M_{hf}, the H_m obtained at different injection frequencies for all the case studies were quite compatible and no significant enhancement on the H_m could be seen. This was shown by the number of case studies obtained for each grade of H_m in Table 1. This might due to inadequate distribution of mixing energy which was governed by other parameters such as the injection position, injection inclination angle [12] as well as crossflow of air into TBIM [13]-[14].

Table 1: Number of case studies obtained for each grade of H_m

Injection frequency	Grades of H_m			
	A	B	C	D
1if	9	12	7	
2if	4	17	7	
4if	8	19	1	

VI. OPTIMISATION OF INJECTION FREQUENCY

To obtain the optimum injection frequency for the best mixing quality, further investigation was conducted for 5if (5-injection/engine cycle) and 7if (7-injection/engine cycle) on selected case studies. As shown in Fig. 7, the M_{hf} at 4if generally showed the lowest value which was closest to $M_{ch4.s}$ relative to the other injection frequencies studied. Thus, 4if gave the best mixing at $M_{ch4.s.}$ For the H_m, on the other hand, it was evident that the H_m obtained at 1if and 4if were comparatively better than those obtained at 2if (Table 1). The former ones had 9 and 8 case studies for Grade A while the latter one had only 4 case studies, as shown in Table 1. Determination of the best H_m obtained between 1if and 4if was rather difficult as they showed nearly the same number of case studies for Grade A. Nonetheless, an obvious variation of the number of case studies obtained for Grade B and Grade C could be seen. Since 4if produced a larger number of case studies for Grade B and a fewer for Grade C, it was claimed to be a better injection frequency for H_m than 1if. Therefore, it could be concluded that the optimum injection frequency of TBIM for the best H_m with M_{ch4} closed to $M_{ch4.s}$ was 4if.

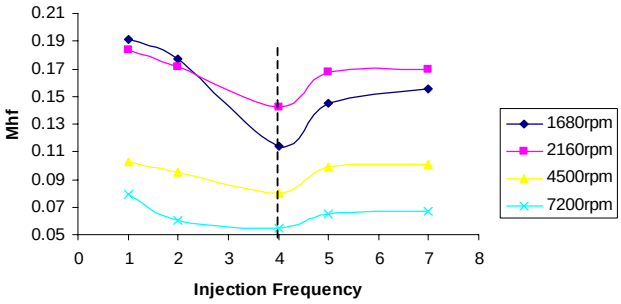

Fig. 7: M_{hf} vs injection frequency at 30 degree throttle opening for different engine speeds

VII. Conclusion

The effect of various injection frequencies on the mixing quality of TBIM in terms of M_{hf} and H_m had been studied in this research. A good mixing was that with M_{hf} closed to $M_{ch4.s}$ and the best H_m at the same time, which was shown by a single contour of M_{ch4} throughout the mixing region during CFD simulation. Although the H_m was not improved remarkably, the M_{hf} was, however, enhanced dramatically with a varying injection frequency. The optimum injection frequency for both M_{hf} and H_m throughout the case studies was found to be at 4if. Future studies on the effect of other parameters such as injection position, injection inclination angle as well as crossflow of air into TBIM should be conducted to further enhance the air-fuel mixing prior to entering the engine.

ACKNOWLEGMENT

We wish to record our sincere gratitude to Universiti Teknologi PETRONAS (UTP) and Universiti Teknologi Malaysia (UTM). Apart from financial support, they made available to us research facilities and resources which were integral to this work. In addition, unstinting technical assistance from Mr. King Ik Piau., Mr Yeap Beng Hi, Mr. Chin Vee Dee, En. Rosdi Baharim, En. Mohd Redhuan Ramli and En. Faizal Ali Othman is greatly acknowledged.

REFERENCES

[1] Papageorgakis, G. and Assanis, D. N. (1998). Optimizing Gaseous Fuel-Air Mixing in Direct Injection Engines Using an RNG Based k-ε Model. *SAE Technical Paper Series*. SAE 980135.

[2] Lacher, S. J., Fan, L., Backer, B., Martin, J. K., Reitz, R., Yang, J. and Anderson, R. (1999). In-Cylinder Mixing Rate Measurements and CFD Analyses. *SAE Technical Paper Series.* SAE 1999-01-1110.

[3] Anderson, R., Yi, J., Han, Z., Yang, J., Trigui, N., and Boussarsar, R. (2000). Modeling of the Interaction of Intake Flow and Fuel Spray in DISI Engines. *SAE Technical Paper Series.* SAE 2000-01-0656.

[4] Dyntar, D., Onder, C. and Guzzella, L. (2002). Modeling and Control of CNG Engines. *SAE Technical Paper Series.* SAE 2002-01-1295.

[5] Yi, J., Han, Z. and Trigui, N. (2002) Fuel-Air Mixing Homogeneity and Performance Improvements of a Stratified-Charge DISI Combustion System. *SAE Technical Paper Series.* SAE 2002-01-2656.

[6] Chang, S. H. *Effect of Injection Characteristics on Throttle Body Injection Mixer for Compressed Natural Gas Motorcycle*. Universiti Teknologi Malaysia. Malaysia: M. Eng. Thesis.

[7] Yi, J., Han, Z., Yang, J., Anderson, R., Trigui, N. and Boussarsar, R. (2000). Modeling of the Interaction of Intake Flow and Fuel Spray in DISI Engines. *SAE Technical Paper Series.* SAE 2000-01-0656.

[8] Fluent Inc. (2001). *Fluent 6 User's Guide*. India: Fluent Documentation Software.

[9] Versteeg, H. K. and Malalasekera, W. 1999. *An Introduction to Computational Fluid Dynamics – The Finite Volume Method*. England: Longman Group Ltd.

[10] Han, Z. and Reitz, R. D. (1995). Turbulence Modeling of Internal Combustion Engines Using RNG k-e Models. *Comb. Sci. & Tech.* Vol (106): 267-295.

[11] Christian, F. 1996. Experimental Study of Mixing Performances Using Steady and Unsteady Jets. In: Cheremisinoff, N. P. ed. *Mixed-Flow Hydrodynamics – Advances in Engineering Fluid Mechanics Series*. Texas: Gulf Publishing Company. 359-381.

[12] Tatterson, G. B. 1994. *Scaleup and Design of Industrial Mixing Process*. United States of America: McGraw-Hill.

[13] Busnaina, A. A. 1985. Transient Predictions of Lateral Jet Injection into Typical Isothermal Combustor Flowfields. *AIAA 23rd Aerospace Sciences Meeting*. January 14-17. Nevada: American Institute of Aeronautics and Astronautics, 1-9.

[14] Ferrell, G. B., Aoki, K. and Lilley, D. G. 1985. Flow Visualization of Lateral Jet Injection into Swirling Crossflow. *AIAA 23rd Aerospace Sciences Meeting*. January 14-17. Nevada: American Institute of Aeronautics and Astronautics, 1-10.